JOURNAL OF MATERIALS SCIENCE **36** (2001) 3933–3939

The structure and mechanical properties of bulk $Zr_{50}Ti_{16.5}Cu_{15}Ni_{18.5}$ metallic glasses

G. ABROSIMOVA, A. ARONIN, D. MATVEEV, I. ZVERKOVA
Institute of Solid State Physics RAS, Chernogolovka, Russia
E-mail: aronin @issp.ac.ru

V. MOLOKANOV
Baikov Institute of Metallurgy and Materials Science RAS, Moscow, Russia

S. PAN, A. SLIPENYUK
Frantsevich Institute for Problems of Materials Science., Kiev, Ukraine

The structure and mechanical properties of bulk $Zr_{50}Ti_{16.5}Cu_{15}Ni_{18.5}$ metallic glasses were studied by X-ray diffraction, scanning and transmission electron microscopy and by measurements of mechanical properties. The transition from heterogeneous to homogeneous deformation was found to occur at 575 K. The crystallization was found to begin in the testing part of the sample earlier than in the part placed in a holder during the mechanical testing. The crystallization leads to the formation of the quasicrystalline phase with $a_0 = 2.54$ Å, hexagonal phase ZrTi(Ni,Cu) and hexagonal phase (Zr_6CoAl_2 type). The difference of the structure in different parts of the sample has been observed and analyzed. The deformation does not effect on the crystallization processes occurring during the tensile testing at this temperature and the crystallization proceeds owing to the self-heating of the samples during the phase transition. The correlation between mechanical properties, structure and fracture surfaces is discussed. *© 2001 Kluwer Academic Publishers*

1. Introduction

An appearance and production of bulk metallic glasses has caused a new interest to amorphous materials. The bulk metallic glasses were produced in a number of systems [1–3]. Bulk metallic glasses show high mechanical properties [4]. They have high tensile fracture strength comparable to that for the melt-spun amorphous ribbons. The partially crystallized amorphous $Zr_{57}Cu_{20}Al_{10}Ni_8Ti_5$ alloy, for example with 40 vol. % of crystalline phase, shows excellent strength with a yield strength of 1700 MPa and a fracture stress of 1780 MPa. However, the ductility of bulk nanocrystalline-amorphous alloys decreases whereas the strength increases with increasing volume fraction of nanocrystalline phase [5].

The Zr-based bulk amorphous alloys belong to the interesting group of bulk metallic glasses because they have very promising mechanical properties. The mechanical properties and structure of the bulk $Zr_{55}Ni_5Cu_{30}Al_{10}$ and nanocrystalline $Zr_{53}Cu_{20}Ni_{10}Ti_5Al_{12}$ alloys were studied recently [6]. The aim of this paper is to study the structure/mechanical property correlation in bulk $Zr_{50}Ti_{16.5}Cu_{15}Ni_{18.5}$ metallic glass.

2. Experimental methods

The bulk amorphous $Zr_{50}Ti_{16.5}Cu_{15}Ni_{18.5}$ alloy was initially prepared by a melt quenching. Pure metals (>99.8%) have been used for the master alloy. The samples were prepared as a ribbon with a section of 0.3 × 3 mm. The bone-like specimens were prepared for tensile tests. Special device was developed in order to prepare a high precision specimens for this testing. The quality of the specimen surface was controlled by light microscopy. In order to avoid the influence of the surface defects on the results of mechanical measurements, specimen surfaces were ground off and polished. Fine abrasive paper was used for the finishing of the specimen lateral faces. The effective length of the specimen operational part was about 12 mm for tensile measurements. Special holders were prepared for tensile testing of the bulk metallic glass. These holders have provided a possibility of placing a PPR-thermocouple in the actual vicinity of the specimen with a good mechanical contact to the substrate; they also have demonstrated a stable behaviour at different testing temperature.

The tensile test were carried out at the temperatures from 293 to 823 K in vacuum. The loading rate was $0.0156\ \mathrm{min}^{-1}$ in the temperature range 293–723 K and it was $0.75\ \mathrm{min}^{-1}$ for the temperature range 773–823 K. The heating rate was about 6 K/min. Some additional experiments were carried out at $T = 685$ and 773 K. In these case the loading rates were $0.05\ \mathrm{min}^{-1}$ and $0.2\ \mathrm{min}^{-1}$, respectively. The temperature gradient was not observed in the tensile furnace.

0022–2461 © *2001 Kluwer Academic Publishers*

The structure of the samples was studied by X-ray diffraction, scanning and transmission electron microscopy. The X-ray diffraction experiments were performed using the SIEMENS D-500 diffractometer using Cu K_α-radiation. The samples deformed at low temperatures (293–648 K) were broken down in two parts. One part was situated in a holder during the mechanical testing, the other one was free (the test portion). The samples deformed at higher temperatures (648–823 K) were divided into three or more parts. The first part was in a holder during the testing as above, the other parts were test portions, it was the parts near and far from the holder. The width of the sample was different in the holder (grip portion) and in the test portion; moreover, the width of the samples was different near and far from holder (specially for high temperatures). This situation was taken into account when the X-ray spectra were analyzed. The samples were studied by differential scanning calorimetry using a DSC 111 SETARAM microcalorimeter as well. The heating rate was 20 K/min.

The electron microscopy investigations were carried out on a JEOL-100 CX and JSM-25S microscopes. Electron microscopy foils were prepared by mechanical polishing with following ion milling. Special holder for the samples after mechanical testing was constructed. The structure of the parts in the holders was studied as a controls. The samples were divided into some pieces if the width increased during the mechanical testing.

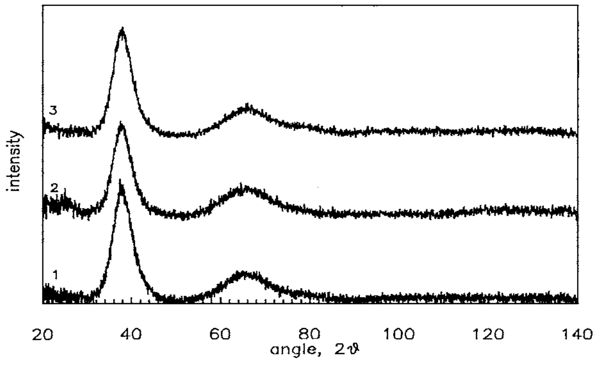

Figure 1 X-ray diffraction patterns of the samples after mechanical testing at 293 K (1), 573 K (2) and 611 K (3).

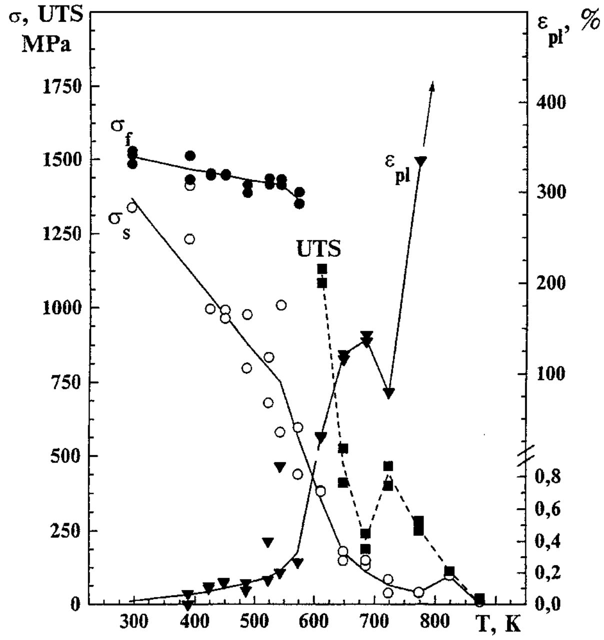

Figure 2 The temperature dependence of UTS, flow and failure stress and plasticity.

3. Results

According the DSC measurements the glass transition temprature T_g is about 600 K. The samples deformed at 293–611 K were amorphous after mechanical testing. The diffraction spectra for the samples deformed

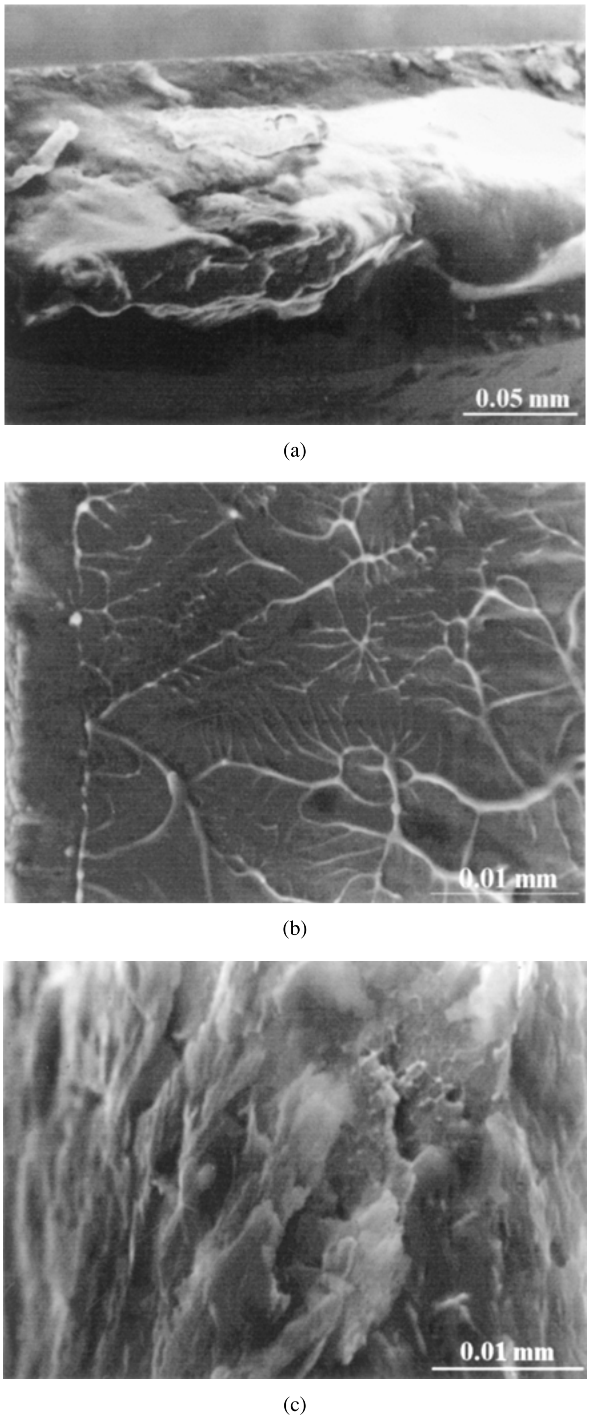

(a)

(b)

(c)

Figure 3 The fracture surfaces of the sample deformed at 293 K (a), 685 K (b) and 723 K (c).

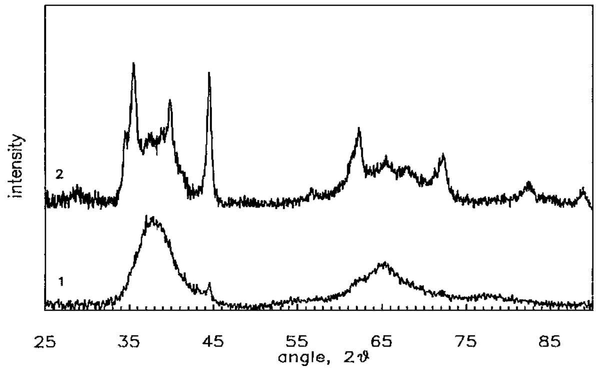

Figure 4 X-ray diffraction patterns of the samples deformed at 685 K (1 - part in a holder, 2 - testing part).

at room temperature, 573 and 611 K contain only the diffuse halos typical for amorphous structure (Fig. 1).

At the tensile experiments the following properties were measured: flow stress $\sigma_s = \sigma_{0.02}$, failure stress σ_f, ultimate tensile stress UTS and plasticity δ. Fig. 2 shows the temperature dependencies of these properties of the alloy. The flow stress and the failure stress monotonously decrease with the temperature increase in the whole studied temperature range. The rate of the flow stress decreasing is higher than the rate of the failure stress decreasing.

A brittle-ductile transition is expected at a temperature below 325 K. The images of fracture surfaces are displayed in Fig. 3 for 293, 685 and 723 K. The fracture surface is shown to change. The river structure was more pronounced when the sample was fractured at the temperatures above 388 K. This structure points to a plastic deformation during the tensile.

The plastic deformation increases sharply above the temperature ~575 K (close to T_g point). The transition from heterogeneous to homogeneous deformation occurs at this temperature. Then the plastic deformation reaches the intermediate maximum of 140% at 685 K. The plasticity decreases (to 80%) at 725 K and it reaches about 335% at 775 K. When the testing temperature was increased from 573 to 685 K, the view of fracture surface changes. The decreasing of typical size of the river structure was observed. Therefore the plastic deformation degree increases with the testing temperature. The fraction of the river structure decreases significantly after the deformation at 723 K (Fig. 3c)

As it was mentioned above, the samples deformed at 293–611 C were amorphous after deformation. The samples deformed at 648 K and higher have crystalline structure (partially or fully crystalline samples, respectively). The loading rate was 0.0156 min^{-1}, it means that the samples was held about 90 min at this temperature during the testing. The crystallization was found to begin in the testing part of the sample earlier than in the part placed in a holder (grip portion). This difference is most pronounced in the samples tested at 685 K (Fig. 4). The grip portion contains predominantly the amorphous phase and the testing portion consists both of amorphous and crystalline phases. So, the crystallization proceeds in effective part to a greater extent than in the holder.

In the test portion of the sample the crystallization proceeds to a greater extent near the fracture region than near the holder. It is more pronounced for the samples deformed at higher temperatures. Fig. 5 shows the X-ray diffraction pattern of the sample tested at 773 K. The reflection separation increases from curve 3 (part

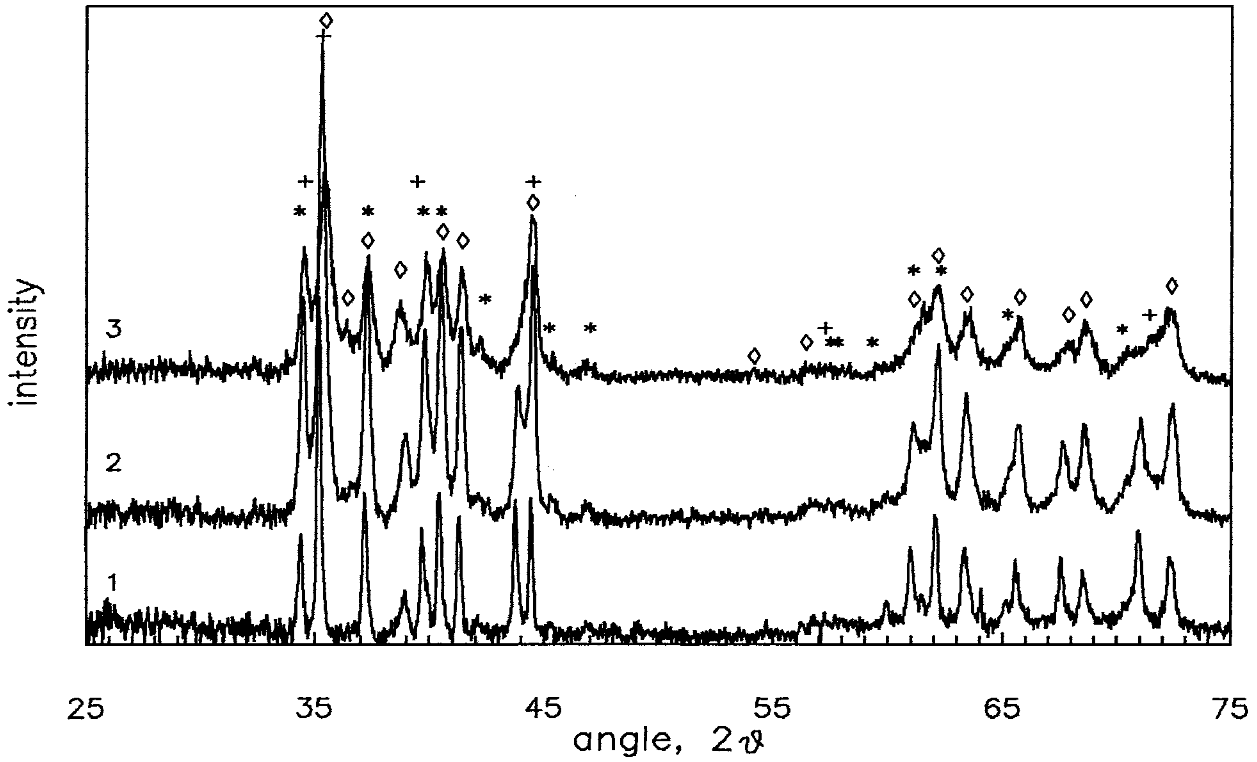

Figure 5 X-ray diffraction pattern of the sample tested at 773 K (1 - testing portion far from the holder, 2 - testing portion near the holder, 3 - part in a holder). The quasicrystalline phase reflections are marked by rhombs, the ZrTi(Ni,Cu) phase reflections are starred and the reflections of Zr_6CoAl_2 type phase are marked by crosses.

in a holder) to curve 1 (testing portion far from the holder).

The X-ray diffraction patterns can be described by following crystalline phases. A quasicrystalline phase with $a_o = 2.54$ Å and a hexagonal phase ZrTi(Ni,Cu) are the main phases. The first phase was observed in Zr-base alloys after crystallization of bulk metallic glasses with different chemical composition [7, 5]. This phase was identified according to the indexing scheme of Cahn [8]. Second phase with hexagonal structure (MgZn2 type, space group $P6_3/mmc$ with lattice parameters $a = 5.24$ Å, $c = 8.54$ Å) was observed as well [9], the lattice parameters change slightly according to chemical composition. The precipitations of Zr_6CoAl_2 type hexagonal phase was observed as well. This phase has a lattice of P62m (189) space group with lattice parameters $a = 7.93$ Å, $c = 3.31$ Å.

Fig. 6 shows the microstructure of the testing part of the sample deformed at 685 K. The dark field TEM image (Fig. 6b) contains a lot of fine crystalline precipitations. The sample part in the holder has an amorphous structure with a few crystalline particles spreaded in the amorphous matrix. The microstructure of the sample deformed at 723 K is displaced in Fig. 7. (The loading rate was 0.2 min^{-1} in this case). The alloy has nanocrystalline structure after this treatment. The size of the nanocrystals is 20–30 nm; they are randomly located in the amorphous matrix.

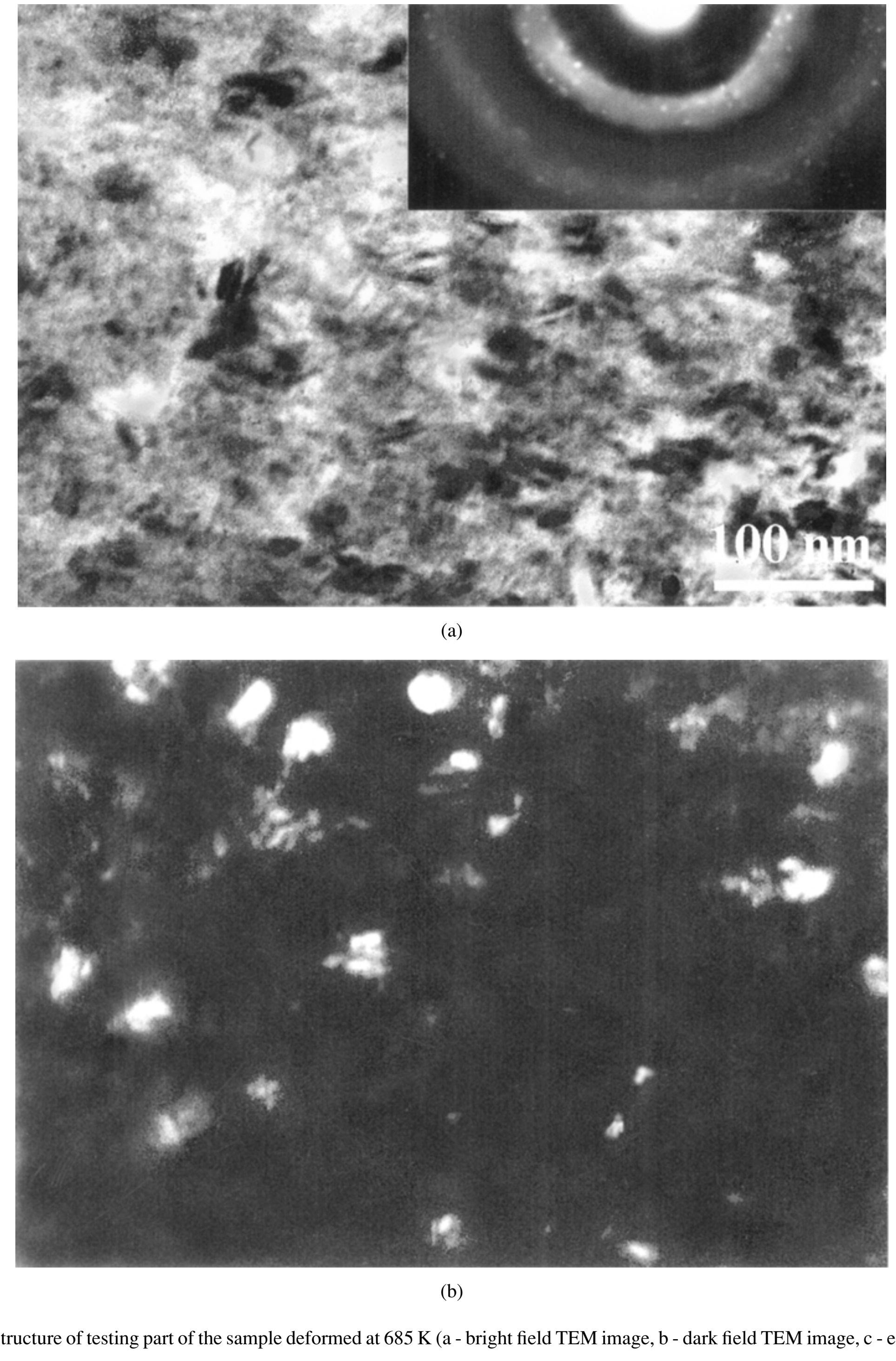

(a)

(b)

Figure 6 Microstructure of testing part of the sample deformed at 685 K (a - bright field TEM image, b - dark field TEM image, c - electron diffraction pattern).

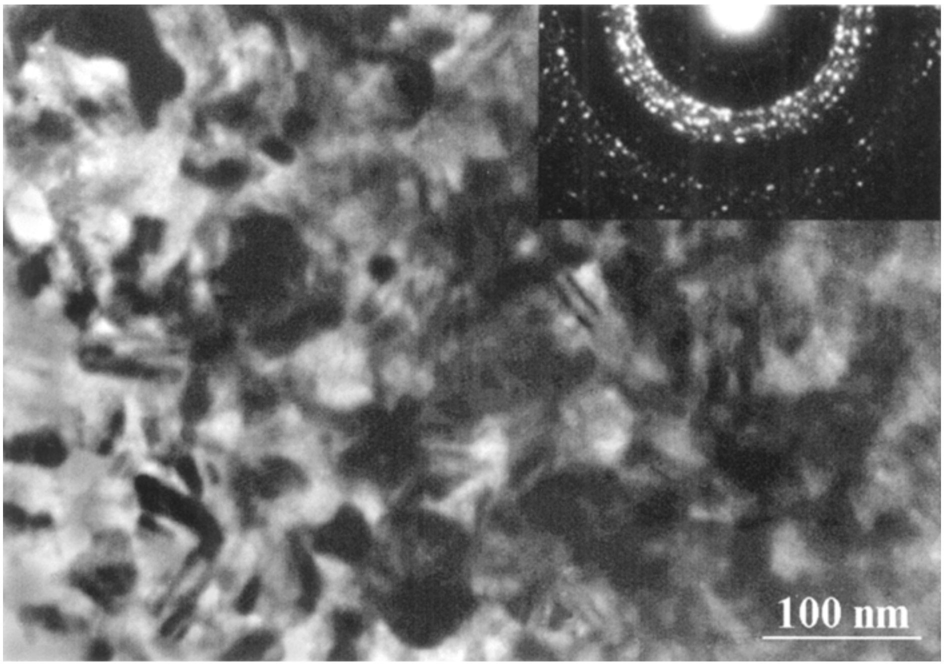

(a)

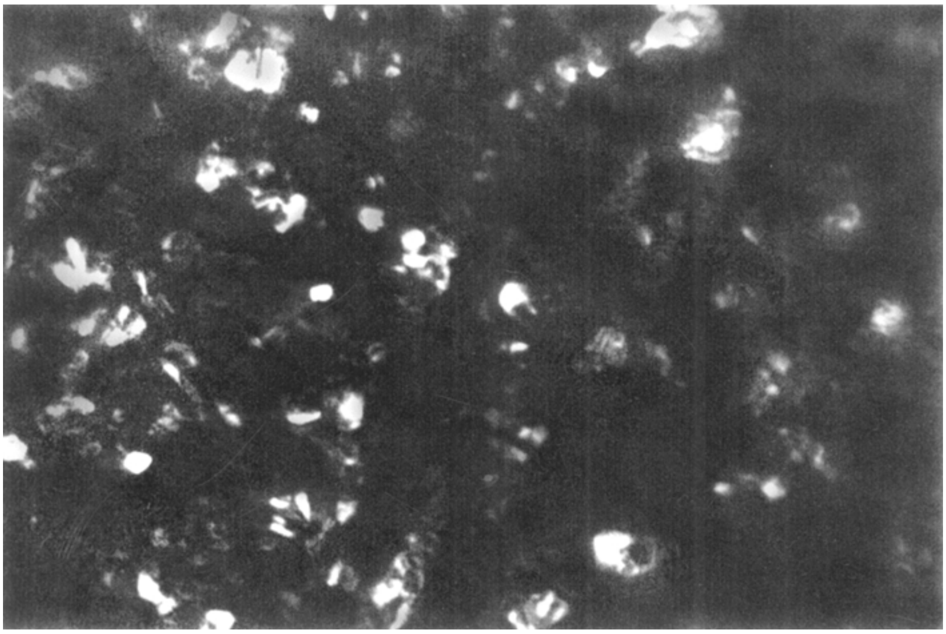

(b)

Figure 7 Microstructure of testing part of the sample deformed at 723 K (a - bright field TEM image, b - dark field TEM image, c - electron diffraction pattern).

After mechanical testing at 773 and 823 K the structure of the alloy is nanocrystalline. The grain size of the crystalline phase does not exceed 50 nm.

4. Discussion

According the experimental data obtained, the temperature range could be divided in three parts. The first temperature range (293–685 K) corresponds the monotonously increasing of the plasticity. The X-ray diffraction and transmission electron microscopy study have shown that the alloy is fully amorphous or it has a very few crystalline precipitations (685 K). So, one may conclude that the mechanical properties are determined by the amorphous matrix in this temperature range. The rise of the plasticity is due to the temperature dependence of the plasticity of the amorphous phase. When the testing temperature is higher than 600 K (T_g), the alloy is in the supercooled liquid state. The deformation occurs by Newton flow in this state, therefore the rise of plasticity appears reasonable.

The structure investigations show that the fraction of the crystalline phase is greater than the fraction of amorphous phase in the second temperature range (685–723 K). In this situation the mechanical properties of the alloy should be determined rather crystalline phase than the amorphous one. Since the plasticity of crystalline phase is low than the plasticity of the amorphous phase

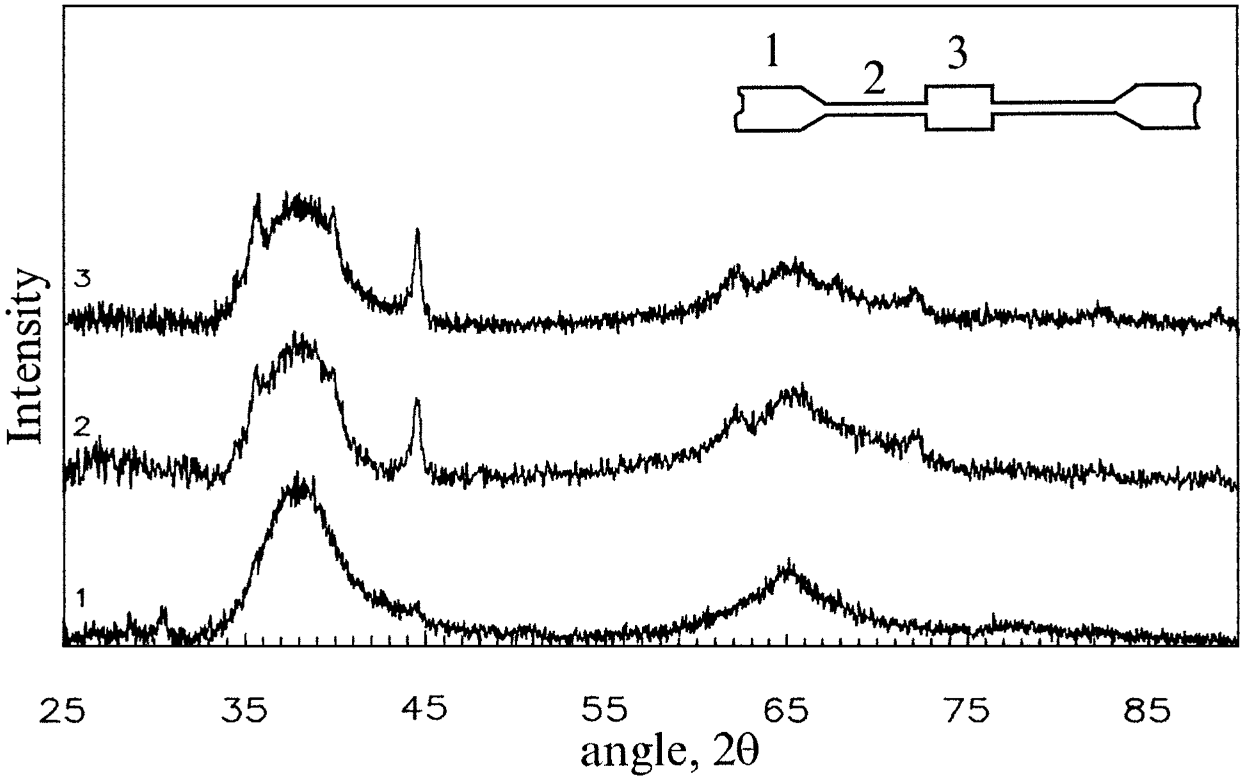

Figure 8 X-ray diffraction pattern of the samples after additional testing at 685 K (1 - part placed in a holder, 2 - test portion, 3 - witness), the shape of the sample is shown in the insert.

in the supercooled liquid state, it could explain the decreasing of the plasticity in this temperature range.

In the last temperature range (723–823 K) the alloy has nanocrystalline structure. So, the rise of plasticity (to 400%) may be connected with the dependence of the nanocrystalline phase deformation on the temperature. In this temperature range the testing temperature is sufficiently high for the increase of plasticity of the nanocrystalline alloy (as superplasticity).

The crystallization was found to begin in the test portion of the sample earlier then in the grip portion (part placed in a holder) when the sample was testing at 685 K. Temperature gradient in the furnace was not observed, that is why the difference in the crystallization extent may be attributed with some reasons.

Firstly, the phase transition takes place at 685 K (the amorphous phase crystallizes). As a result, crystallization heat releases and the temperature of the sample increases (a self-heating of the sample occurs). Since, the releasing heat is removing through the holders and the deforming part of the sample has sufficiently less cross-section than the part in the holders, heat removing from the test portion is hindered. Hence, the temperature of the deformed part of the sample can exceed the temperature of the grip portions.

Secondly, the test portion has deformed significantly. Therefore the difference of the structure in different parts of the sample may be connected with a high deformation of the test portion of the sample.

Some additional experiments were carried out in order to understand which of two factors mentioned above makes the main effect on the crystallization process. New samples were prepared for the mechanical testing; they have a shape of twin-bone (Fig. 8, insert). The wide part in the center of the samples was used as a witness (it does not deformed practically during the tensile deformation). The loading rate was 0.05 min^{-1}. The samples were in a furnace about 60 min. Fig. 8 shows also the X-ray diffraction pattern of the sample after the testing at 685 K. The sample part placed in a holder at the testing remains an amorphous structure (curve 1), the test portion (curve 2) and the witness are partially crystallized. The crystallization in the witness proceeds to a greater extent than in the test portion although the witness does not deform. So, one may conclude that the deformation does not effect on the crystallization processes occurring during the tensile testing at this temperature and the crystallization proceeds owing to the self-heating of the samples during the phase transition.

Since the releasing heat is removed from the witness through the test portion, the heat removing from this part of the sample is still further hampered. Therefore one should expect that the temperature of the witness will be higher and the crystallization processes will be more complete in this region, as it was observed.

When the Fig. 4 is compared with Fig. 8, it is apparent that the test portion of the sample deformed at the loading rate 0.0156 min^{-1} (Fig. 4 curve 2) has more crystalline phase than testing part of the sample with the loading rate of 0.05 min^{-1}. It should be noted that the sample was in a furnace during 90 min in the former case and during 60 min in the second case. Therefore, the phase transformation has proceeded to a greater extent at the lower loading rate because of a longer "annealing".

5. Conclusions

1. Mechanical properties of $Zr_{50}Ti_{16.5}Cu_{15}Ni_{18.5}$ bulk metallic glass were studied during tensile tests at elevated temperatures. The plastic deformation was found to increase above the temperature ∼575 K, it reaches the intermediate maximum of 140% at 685 K. Then the plasticity decreases (to 80%) at 725 K and it increases again to 335% at 775 K. The transition from heterogeneous to homogeneous deformation was observed at a temperature about 575 K.

2. The structure of bulk metallic glass has been studied after mechanical tests. The samples deformed at 293–611 C were amorphous after deformation. The samples deformed at 648 K and higher have partially crystalline or crystalline structure.

3. The crystallization leads to the formation of the quasicrystalline phase with $a_o = 2.54$ Å, hexagonal phase ZrTi(Ni,Cu) ($MgZn_2$ type, space group $P6_3/mmc$ with lattice parameters $a = 5.24$ Å, $c = 8.54$ Å) and hexagonal phase (Zr_6CoAl_2 type), P62m (189) space group with $a = 7.93$ Å, $c = 3.31$ Å.

4. The alloy has nanocrystalline structure after the tensile testing at 723 K. The size of the nanocrystals is 20–30 nm; they are randomly located in the amorphous matrix.

5. The crystallization begins in the testing part of the sample earlier than in the part placed in a holder. This difference is most pronounced in the samples tested at 685 K.

6. The self-heating of the samples was observed during the crystallization at the tensile testing.

Acknowledgment

The financial support of INTAS (grant 96-2126) and RBRF (grant 99-02-17459) is gratefully acknowledged. The authors are grateful to Prof. U. Köster, Prof. L. Battezzati and Prof. M. Baricco for helpful discussion.

References

1. A. INOUE, T. ZHANG and T. MASUMOTO, *Mater. Trans. JIM* **33** (1990) 177.
2. A. PEKER and W. L. JOHNSON, *Appl. Phys. Lett.* **63** (1993) 2342.
3. A. INOUE, *Mater. Trans. JIM* **36** (1995) 866.
4. L. Q. XING, D. M. HERLACH, M. CORNET, C. BERTRAND, J.-P. DALLAS, M. H. TRICHET and J.-P. CHEVALIER, *Mater. Sci. Eng.* **A226-228** (1997) 874.
5. L. Q. XING, J. ECKERT, W. LÖSER and L. SCHULTZ, *Appl. Phys. Lett.* **74** (1999) 664.
6. C. FAN, C. LI, A. INOUE and V. HAAS, *Phys. Rew. B*, **61** (2000) R3761.
7. U. KÖSTER, J. MEINHARDT, S. ROOS and H. LIEBERTZ, *Appl. Phys. Lett.* **69** (1996) 179.
8. J. W. CAHN, D. SHECHTMAN and D. GRATIAS, *J. Mater. Res.* **1** (1986) 13.
9. S. SPRIANO, C. ANTONIONE, R. DOGLIONE, L. BATTEZZATI, S. CARDOSO, J. C. SOARES and M. F. DA SILVA, *Phil. Mag.* **76B** (1997) 529.

Received 27 June 2000
and accepted 3 April 2001